Pattern Recognition Letters 21 (2000) 531–548

Registration of CT and MR images of Alzheimer's patient: a shape theoretic approach

M. Bhattacharya, D.D. Majumder *

Electronics % Comm. Sciences Unit, CSU, Indian Statistical Institute, 203 B.T. Road, Calcutta 700035, India

Abstract

In this paper, we present briefly the generalised theory of shape as developed by Majumder (Majumder, D.D., 1995. A study on a mathematical theory of shapes in relation to pattern recognition and computer vision. Indian Journal of Theoretical Physics 43 (4), 19–30) and apply the same to registration of multimodal medical images. We have conducted the experiment of registration using T_1/T_2 weighted MR and CT imaging modalities of ventricular region (region of interest (ROI) in Alzheimer's disease (AD)) of brain of an Alzheimer's patient. The control points on the concavities present in the contours are chosen to re-project ROI from the respective modalities in a reference frame. The best matching and registration are achieved by minimising an error factor.

Keywords: Mathematical theory of shape; Affine and projective transformation; Registration of multimodal images

1. Introduction

The registration of images is of great importance not only in the case of medical images of different modalities of clinical interest but also as an interesting problem in computer vision. The perception of shape rather than color and texture plays an important role in human visual learning process as well as in pattern recognition, scene analysis and artificial vision system by computer. Shape identifies both 2D outline and 3D surface of an object. One of the present authors and his co-authors in some earlier papers (Parui and Majumder, 1982; Banerjee et al., 1994; Majumder and Bhattacharya, 1997, 1998) presented a mathematically rigorous definition of shape, developed 2D and 3D shape metrices (Dutta Majumder's shape metric) and applied them for several pattern recognition and scene analysis problems (that are not relevant here), and also in image registration problem (Banerjee et al., 1995). In this paper, we briefly present a recent contribution on a generalised mathematical theory of shape (Majumder, 1995) which we attempt to apply in medical image registration. Kendall (1989), Bookstein (1986) and Dryden and Mardia (1998), have also attempted a Statistical Theory of Shape in recent times.

In the case of multimodal medical imaging the absence of robust automatic registration algorithm is standing in the way of entering this techniques in diagnostics and therapeutic planning though there is no resistance from the clinicians in using the

* Corresponding author. Fax: +91-33-577-6680.
E-mail address: ddm@isical.ac.in (D.D. Majumder).

technology. In medical image registration two images of the same object of two modalities or of same modality taken at different times is to be aligned as accurately as possible. The present paper concerns registration of CT, T_1 and/or T_2 weighted MR images of brain (axial section) of a patient suffering from Alzheimer's Disease (AD) as part of an investigation being carried out by the authors (Majumder and Bhattacharya, 1998, 1999; Banerjee et al., 1995) to develop a knowledge based framework for combining different modalities of medical imaging such as CT, MR, PET, SPECT and USG whichever is relevant for a particular pathological investigation. In the present experiment, we have used image data of a patient suffering from AD which is a common degenerative disease of the brain (Arai and Kobasaki, 1983; Creasay and Schwartz, 1986). It is well known that the ventricular region of brain is affected due to AD. The deformation of the ventricle of AD patient indicate the overall prognosis of the disease (Arai and Kobasaki, 1983; Creasay and Schwartz, 1986) and is considered as the region of interest (ROI) from where the features are to be detected for diagnosis.

Applications of PET and SPECT imaging are expected to shed more light (Medical Imaging International Journal, 1996) but these techniques are costly and not available for such clinical or research studies to us as yet. Our attempt is to improve the diagnosis and treatment planning with CT and MR images that are normally available in hospitals. When the ROI of any diseased part of human body is captured by different imaging sensors (like CT, MR, PET, SPECT, USG) it is desirable to establish the point to point correspondences and finally to match the relevant multimodal images of the ROI. Our approach is valid for registration of images preferably taken in a contemporary period but also for temporal periods to study the progress of the disease when re-registration is advised.

We have experimented with CT and MR modality and in both cases cavities are well delineated. All types of sensors are not expected to perform equally well for all types of structures, but it should be possible to find some features, which are delineated by the two relevant sensors in a particular case for the purpose of registration.

Earlier works (Thirion et al., 1992; Van den Elsen, 1993, 1994; Hill, 1993; Shashua and Navab, 1994; Grimson et al., 1994; Martin et al., 1994) depict the registration of CT and MR images by a semiautomatic method where the local and global transformations are used depending on the number of structures of interest. Affine transformation and matching are proposed in (Landan et al., 1985; Shashua and Navab, 1994). In the paper (Grimson et al., 1994) an automatic registration is suggested for 3D clinical data from segmented CT and MRI reconstruction in order to guide the neuro-surgical procedures. Detection of symmetry for affine images using shape has been reported in (Mukherjee et al., 1994).

In this context we may refer the comparison and evaluation of retrospective intermodality brain image registration techniques as it is described in (West et al., 1997). A target registration error (TRE) has been defined as a true representation of the distance between the actual and estimated positions of targets within the cranial cavity. A complete evaluation of retrospective techniques based on their TRE at different landmark locations within the brain has been performed using fiducial markers (West et al., 1997) as a 'gold standard'. The two registration tasks have been evaluated between CT and MR and other between PET and MR. The measurement of error was made with respect to gold standard over a volume of interest (VOI). Fiducial markers are filled with an aqueous solution designed to be bright in CT and MR images and also for PET. An intensity-based centroid has been calculated for each marker using the localisation technique, and that the determination of this topic is called fiducial localisation. This iterative knowledge-based technique automatically finds the lowest threshold such that an object formed from voxels whose intensities are higher than the threshold and that are three dimensionally connected to a selected voxel is neither too large nor too small to be a marker when these markers are used to register images. In registration of CT and MR, and PET and MR the rotation and translation parameters are calculated of a rigid body transformation that

minimises the mean square distance between the corresponding fiducials in two images. The retrospective registration was performed in parallel at several sites. Some methods were used applicable only to CT and MR and some are applicable to PET and MR registration and some are suitable for both the cases. Barillot and Lemoine (see e.g. West et al., 1997) used a two-stage technique both for CT and MR and PET and MR registration. The first step is to perform an approximate registration of objects. The second stage is the application of a multiresolution Powell algorithm, which minimises the Euclidean distance between the two surfaces given by a chamfer mask. Twelve such registration techniques have been attempted in different workstation and reported (West et al., 1997).

A recent approach of medical image registration using the mutual information measure (Thevenaz and Unser, 1997; Collignon et al., 1995; Well et al., 1995; Bhattacharya and Majumder, 1999) along with the use of Parzen window estimator for optimisation has been reported in (Thevenaz and Unser, 1997). The optimisation criteria of mutual information measure can be successfully used for multiresolution image registration. According to this idea a framework is developed where the images have to be presented as a continuous B-spline polynomial together with the use of Parzen window estimator. According to this concept an image pyramid has been computed to get the optimiser in a multiresolution framework.

In (Majumder and Bhattacharya, 1998; Banerjee et al., 1995; Hill, 1993) a number of point landmark-based registration methods have been proposed. In (Majumder, 1995; Majumder and Bhattacharya, 1998, 1999; Banerjee et al., 1995) shape-based semi automatic registration methods have been suggested using geometric invariance properties that comprise two approaches. In the first approach, the concept of shape metric, shape distance function, shape similarity measure between the two shapes, have been established (Parui and Majumder, 1982; Banerjee et al., 1994; Majumder and Bhattacharya, 1997). This approach has been used to find the match/mismatch between the shapes of the two images by defining a shape distance measure, which satisfy all the metric properties. The second approach is the generalised theory of shape (Majumder, 1995) where from two given sets of landmark points in the respective images we have derived a coordinate transformation linking the two sets. In the present paper, we have adopted the second approach to register the T_1 and T_2 weighted MR and CT images of brain of an Alzheimer's patient in a common reference frame and to find the 'best matching'. The first approach provides a measure of match/mismatch between different shapes without registering the images whereas using the generalised approach the images are registered in a reference frame and the goodness of matching is determined by selecting landmark points along the concavity of the contour of the ROI. From the mathematical point of view the first approach is a special case of the second approach or generalised approach.

There are various physical causes of image degradation which cannot be avoided in the imaging process that results in distortion and noise for which there are various appropriate image enhancement, restoration and filtering techniques that need to be adopted. The most important preprocessing task prior to the registration of the images is to do the segmentation of original images into ROIs. The edges are extracted from the segmented region by detecting the points of transition between two homogeneous areas. Among the various approaches to segmentation we have adopted Canny-edge-detector (Canny, 1986) to extract the boundary pixel chains of the edges and vertices. To locate the corner points, vertices and the points of maximal curvature the convex hull (Preparata and Ianshamos, 1985) method is employed on the extracted contour at the output of the detector. Canny's segmentation algorithm is chosen as it optimises the following criteria: (a) low error rate, which is achieved by maximum signal to noise ratio and (b) better localisation of the edge points. Here the input image is convoluted by the Gaussian smoothing filter having some smoothing factor. By choosing the double thresholding values the required images are obtained and finally this algorithm performs the edge linking as a by-product of thresholding. We shall discuss about

our preprocessing and segmentation algorithms in some detail in Section 4.

2. Image registration

In this section, we shall discuss the two methodologies of image registration using the concept of mutual information and the second one is the generalised shape-based registration of images as developed and used in this paper.

2.1. Image registration using the concept of mutual information

The mutual information between the two images can be regarded as a statistical tool to measure the degree to which one image can be predicted from the other using Kullback–Leibler measure (Thevenaz and Unser, 1997) that was proposed as a registration criterion by some authors (Thevenaz and Unser, 1997; Collignon et al., 1995; Well et al., 1995; Bhattacharya and Majumder, 1999) including medical image registration. This measure is also referred to as relative entropy. The mutual information I between an image m and an image n defined from 2D probability distribution of intensities as

$$\boldsymbol{I}(m,n) = \sum_{m\in M}\sum_{n\in N}\boldsymbol{I}\{m,n\}\log p(m\cdot n)/p(m)p(n).$$

We take M as the set of intensities in image m and N as the set of intensities in image n present in the region of overlap of two modalities. Otherwise this can be presented in terms of information present in image m as $H(M)$ and in image n as $H(N)$ and in combined image as $H(M,N)$

$$\boldsymbol{I}(M:N) = H(M) + H(N) - H(M,N).$$

To maximise the mutual information the combined image has to be minimised. Since the idea of mutual information criterion comes from statistical dependence between two images the criterion would be optimised for a suitable geometric transformation for which the dependence between the two images might be maximised. Every pixel of the images contributes to the mutual information criterion. For a test image $f_T(\mathbf{x})$ to be aligned to a reference image $f_R(\mathbf{x})$, when the images are defined on a continuous domain $\mathbf{x} \in \mathbf{V}$. The coordinates x_i, y_i are samples of $\mathbf{V}$. Let $g(\mathbf{x} : v_1, v_2, v_3, \ldots)$ be some geometric transformation with associated parameters $\boldsymbol{v} = (v_1, v_2, v_3, \ldots)$. The problem of image registration is to find the set of parameters for best correspondence of reference image with the test image. The levels of intensities to the test and reference images are supposed to be L_T and L_R. Let w be a separable Parzen window. The joint discrete Parzen probability is defined as

$$p(\iota,\kappa,\boldsymbol{v}) = \alpha(\boldsymbol{v})\sum w(\iota - f_T(g(x_i,\boldsymbol{v})))w(\kappa - f_R(x_i)),$$

where α is the normalisation factor that measures $\sum p(\iota,\kappa) = 1$ and, where $\iota \in L_T$ and $\kappa \in L_R$. The mutual information between the transformed image and the reference image is given by

$$I(\boldsymbol{v}) = -\sum\sum p(\iota,\kappa,\boldsymbol{v}) \times \log_2\{p(\iota,\kappa,\boldsymbol{v})/p_T(\iota,\boldsymbol{v})p_R(\kappa,\boldsymbol{v})\},$$

where $p_T(\iota,\boldsymbol{v})$ and $p_R(\kappa,\boldsymbol{v})$ are marginal discrete probabilities related to test image and reference image. An image can be expressed through a set of samples $f_i = f(x)$ which is discrete in nature spaced on a cartesian grid. But to perform any geometric transformation the function should be smooth and continuous on the other hand one can interpolate an image to provide the link between the samples f_i and their location x_i. Hence B-spline representation of the image model is to be considered to have the advantage of being smooth functions with explicit derivatives. The quality of the registration increases by increasing the degree of the model. The lowest possible degree $n = 0$ is called the nearest neighbour. Better optimisation is achieved by increasing the degree n of the model. Thus the final solution can be attained starting from a coarser level to some finer level.

To get the optimum value of the mutual information $\boldsymbol{I}$ with respect to the parameter of geometric transformation $\boldsymbol{v}$ considering the multi resolution aspect $\boldsymbol{I}$ is expanded by the Taylor series where for optimal solution gradient of $\boldsymbol{I} = (\delta\boldsymbol{I})$ should be zero. In such condition the dependence between the test image and the reference image is complete. This is a situation of ideal registration

where exact mapping occurs. The marginal discrete probabilities for both test and the reference images are same.

2.2. A generalised theory of shape: application to registration and matching

As stated earlier so far developed shape-based methodologies follow two approaches: (A) to characterise shape differences via an analysis of metric components and (B) from the two sets of landmark points to derive a coordinate transformation linking the two sets and an analysis of its properties. In both the approaches shape is defined as an equivalence relation and is invariant of translation, rotation and scaling (Majumder, 1995; Parui and Majumder, 1982; Majumder and Bhattacharya, 1997; Banerjee et al., 1995). For the sake of clarity and completeness a brief comparison between the two approaches will be in order.

2.2.1. The concept of shape metric

According to the first approach the degree of matching or similarity between shapes that can be measured by using the mathematical theory of shape and from which concept 2D shape distance function is derived (Parui and Majumder, 1982; Banerjee et al., 1994; Majumder and Bhattacharya, 1997). This theory can be further extended to 3D problems from which the concept of 3D shape metric and a distance measure is developed (Parui and Majumder, 1982; Banerjee et al., 1994). The two objects have the same shape if one is a translation, dilation and rotation of the other. Using the concept of shape metric the shape matching is done by normalising an object in terms of its position, size and orientation. After normalisation the mismatch is measured in terms of shape distances between two objects where all the metric properties are retained. Shape is described on the basis of its structural features using certain chain codes. The two reference points are obtained by the intersection points of the major axis with the contour of the region are invariant under translation, rotation and dilation of the region. From these two reference points the strings of directional codes describing the border are extracted. The distance between the two shapes is defined in terms of these strings. Here shape is defined as an equivalence class generated by $\boldsymbol{R}$ in R where $\boldsymbol{R}$ is an equivalence relation in R such that two regions A and $B \in R$, if the region A can be obtained from the region B through translation, rotation and dilation. Two regions A and B have the same shape if and only if $(A,B) \in \boldsymbol{R}$. A 'region' is a closed, bounded and connected subset of the Euclidean plane $\mathbb{R}^2$. The similarity measure μ between the two shapes is defined in terms of difference in distance function measure $\boldsymbol{D}$ between the two regions as $\mu = 1 - \boldsymbol{D}$. Higher values of μ indicate higher degree of matching or similarity in shape between the two regions.

2.2.2. Generalised theory of shape

In the second approach of shape-based landmark (geometric invariance) detection and registration method, Majumder has defined shape to refer to those geometrical attributes that remain unchanged when the figure is translated, rotated and scaled (Majumder, 1995).

Affine and projective invariance relations are used to re-project the region of interest into another view. The visual recognition is achieved by alignment and the geometrical invariants extracted from the concavities present in the ROI. The concept of canonical frame (Majumder and Bhattacharya, 1998; Banerjee et al., 1995; Mundy and Zisserman, 1992) is introduced in transformation of a set of coordinates and to match the segmented regions to be registered. A canonical system is defined with non-homogeneous coordinates. A few set of points or the control points are determined in this frame and the corresponding invariants of an appropriate concavity of the image are mapped on them to map all the coordinate points of the segmented contour in this reference frame. Similar planar contour segments are brought into correspondence under affine or projective transformation depending on the projection model when the shape of the contours are fully characterised by the type of transformation as (a) the search of correspondence between points of two images or one image and its model and (b) extraction of features.

In this model, affine and projective transformation are grouped on the basis of the degrees of

freedom (DOF). As a result more features are associated to compute invariants for higher degree of freedom to improve the matching between the planar contour. The affine transformation needs at least three coplanar points and six DOF to construct invariants and for projective case at least four coplanar points are required, whereas Euclidean group requires only two points to construct an invariant distance.

Definition 1. A geometrical figure in $\mathbb{R}^3$ space consists of N number of landmark (control points) and can be represented by a matrix $N \cdot K$. These landmark points specify the identification and comparison among the interspaces and intraspaces of biological homology and are corresponding invariants for registration. If two geometrical figures F and F' are made congruent by a rigid body transformation can be expressed as

$$F' = \gamma F R + J_N \tau^t, \tag{1}$$

where R specifies a $K \cdot K$ rotation matrix and τ specifies a $K \cdot 1$ translation matrix. Where J_N is the N vectors of ones. This translation rotation pair is a transformation acting on Euclidean group in $\mathbb{R}^3$ space considering shape to be an equivalence class (Majumder, 1995; Parui and Majumder, 1982).

We may compare F and its transformed form F' in transformation coordinate. If the two shapes F and F' have the same shape after transformation such that $F \sim F'$ they are related by the equation $F' = \gamma F R + J_N \tau^t$, where γ is a scalar quantity and γ is greater than zero. The triplet (τ, γ and R) specifies the translation, scaling and rotation component of the similarity transformation from F to F'.

Let us now consider a coordinate transformation via which one set of landmarks can be mapped onto the other for a closed match. Using a Taylor series expansion the coordinate transformation can be expressed as a polynomial series in the coordinates. The series can be split up into two parts, an affine part (lower part) and a non-linear part. The point is that the coordinate transformation is in some sense a measure of 'shape difference' or the shape difference can be characterised via the coordinate transformation (Majumder, 1995).

Let x_i, y_i and x_i', y_i', be the two sets of landmarks for $i = 1, 2, \ldots, n$. By landmarks we mean some conspicuous features of the structures that indicate some events marking some stage or stages in the development of the structure and they are invariant under translation, rotation and scaling. In present problem the landmark points are detected on a chosen concavity as the point of maximum curvature by convex hull method (Preparata and Ianshamos).

The transformation considered can be expressed as

$$x_i' = a_0 + a_1 x + a_2 y + a_3 x^2 + a_4 xy + a_5 y^2 + \cdots, \tag{2a}$$

$$y_i' = b_0 + b_1 x + b_2 y + b_3 x^2 + b_4 xy + b_5 y^2 + \cdots, \tag{2b}$$

where A is defined as

$$A = \begin{pmatrix} a_0 \\ a_1 \\ a_2 \\ \vdots \\ a_n \end{pmatrix} \tag{3a}$$

and B is defined as

$$B = \begin{pmatrix} b_0 \\ b_1 \\ b_2 \\ \vdots \\ b_n \end{pmatrix}. \tag{3b}$$

It is clear that the coefficients a_0, a_1, a_2 in A and b_0, b_1, b_2 in B are related to the affine part and the higher order terms a_3, a_4, a_5 and so on in A and b_3, b_4, b_5 and so on in B are related to the non-affine (non-linear) part of the transformation equations (2a) and (2b). For the closest match the least square solution for coefficient matrix A and B of the transformation are searched by minimising the expression $\|NA - X\|^2 = 0$ where N is given by

$$N = \begin{pmatrix} 1 & x_1 & y_1 & x_1^2 & x_1y_1 & y_1^2 \\ 1 & x_2^2 & y_2 & x_2^2 & x_2y_2 & y_2^2 \\ \vdots & \vdots & \vdots & \vdots & \vdots & \vdots \\ 1 & x_n & y_n & x_n^2 & x_ny_n & y_n^2 \end{pmatrix} \tag{4}$$

from the definition of the above expression the corresponding solutions for A and B are given by:

The required solution for A is given by

$$A = (N^{\mathrm{T}}N)^{-1}N^{\mathrm{T}}X \tag{5a}$$

and the required solution for B is given by

$$B = (N^{\mathrm{T}}N)^{-1}N^{\mathrm{T}}Y, \tag{5b}$$

where

$$X = \begin{pmatrix} x_1' \\ x_2' \\ \vdots \\ x_n' \end{pmatrix} \tag{6a}$$

and

$$Y = \begin{pmatrix} y_1' \\ y_2' \\ \vdots \\ y_n' \end{pmatrix}. \tag{6b}$$

At least three control points are required to fit two linear polynomials and from the least square solution the control points are selected for best fit for which the higher order coefficient terms in the polynomial are minimum. However, we can improve the matching by including sufficient terms in the polynomial.

In contour matching in canonical frame the affine transformation and projective transformation are derived from this generalised theory as two special cases. In affine case to transform a contour in canonical frame the three landmark points on the chosen concavity are the entry, exit and height points of Fig. 1(a) and six parameters are associated by 3 DOF. For the projective case to transform a contour in the canonical frame the four corner points are the landmark points where eight parameters are associated by 4 DOF, Fig. 1(b). Here we may point out that Euclidean case also is a special case of the generalised theory.

2.2.3. Detection of control points in affine and projective plane

If we consider two sets of landmarks and one set is mapped onto the other by appropriate transformation like affine or projective the two shapes are same if they are exactly superimposed. If exact superposition is not possible a closest match can be found (Majumder, 1995). The input-to-output and vice versa mapping may be computed by fitting a function. Control points are features located in the input image and whose location in the final output is known. If the registration is being done to force the input image to align with a reference image, the control points are features located both in the input and reference images. Let us now consider the affine and the projective transformation via which one set of landmarks can be mapped onto the other.

2.2.3.1. Affine transformation. The basic step of affine transformation is to deform an object or a plane non-rigidly where the invariants in affine plane remains unaltered. The algorithm related to affine transformation superposes two surfaces in 3D objects or two planar contours of the ROI in 2D plane.

Definition 2. For a set of points in $\mathbb{R}^2$ the corresponding transformation in affine plane say $P : \mathbb{R}^2 \to \mathbb{R}^2$. Each point m in one image is translated to corresponding transformed points

$$m' = \boldsymbol{C}m + \boldsymbol{d}, \tag{7}$$

where $\boldsymbol{C}$ is a nonsingular 2×2 matrix and $\boldsymbol{d}$ is the translational vector. In the required canonical frame the non-colinear triplet of model points are transformed to coordinate position $(-100, 0)$; $(100, 0)$; $(0, 100\sqrt{3})$. Here $\boldsymbol{d} \in \mathbb{R}^2$ for all $m \in \mathbb{R}^2$.

The affine transformation allows to map all the points m of the boundary of the objects in the plane P to of the transformed plane P_1 for all $m \in P$, and all $m' \in P_1$. From the collection of m points $(m_1, m_2, m_3, \ldots, m_l) \in \mathbb{R}^2$ where a set of three points in m which are non co-linear and

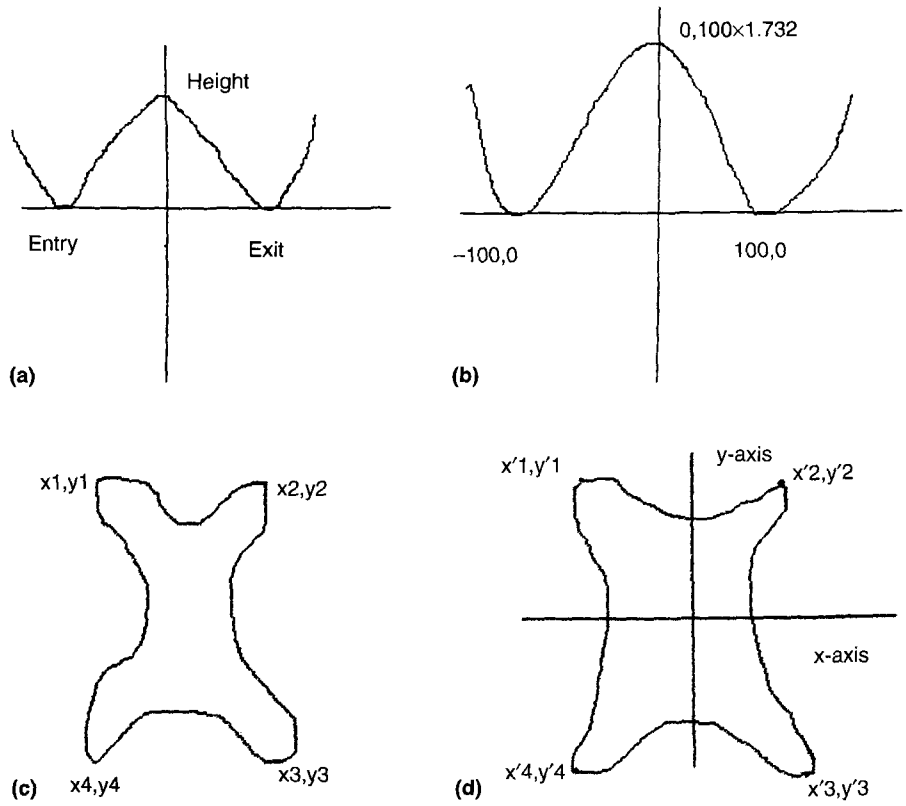

Fig. 1.

uniquely define an affine transformation. The three non-colinear points are p_1, p_2, p_3 and the corresponding transformed points be p'_1, p'_2, p'_3 then there exists affine transformation which maps $\mathbb{R}^2 \rightarrow \mathbb{R}^2$.

If p_0 be the origin then a basis vector v_i can be defined as $v_i = p_i - p_0$ for $i \in (1,2,3)$. The three distinguished points on the planar contour are termed as entry, exit and height points on the chosen concavity.

The generalised expression for the transformation matrix determines the projectivity from these basis points pair x_t, y_t to map the points in the canonical frame where x_c, y_c are the corresponding control points.

The required transformation matrix is given by

$$\begin{pmatrix} x_c \\ y_c \end{pmatrix} = \begin{pmatrix} p & q \\ s & t \end{pmatrix} \begin{pmatrix} x_t \\ y_t \end{pmatrix} + \begin{pmatrix} r \\ u \end{pmatrix}. \tag{8}$$

The six DOF are specified by the parameters p, q, r, s, t, u in affine plane to map the chosen concavity in the canonical frame. Here x_t and y_t are detected from convex hull method and are the hullpoints of the corresponding concavity of the contour and x_c and y_c are the corresponding control points in the canonical frame. Here six DOF are specified by the six parameters in the above equation related to translation and rotation. These parameters are computed to get all the transformed coordinates of the corresponding contour in canonical frame for both the images.

2.2.3.2. Projective transformation in homogeneous coordinate system

Definition 3. Any planar transformation of homogeneous coordinates define a projective transformation of the projective plane. A point in the

projective plane can be presented by three coordinates as $(x_1, x_2, x_3)^T$ and are called homogeneous coordinates. In the projective plane of three homogeneous coordinates the transformation is expressed by a 3×3 matrix and the eight degrees of freedom are specified by the parameters in a nine dimensional space defined by all the matrix elements.

A projective transformation can be represented between two planes as

$$x = TX^T. \tag{9}$$

By definition a (2D) point (x,y) could be transformed to homogeneous space $(tx, ty, t)$for $t \neq 0$. Generally speaking it is a transformation from x to $(x+1)$ space where the relationship between the Euclidean and homogeneous space is given by $x = (tx/t)$; $y = (ty/t)$ for 3D homogeneous coordinate (tx, ty, t), $t \neq 0$ of the 2D point x,y. Homogeneous coordinates are actually used to represent a point where parallel lines tend to 'meet'. While we define two parallel lines meet at infinity under perspective transformation, two parallel lines actually meet at a point or appear to meet at a point and in many image processing, computer vision applications we need to calculate that coordinate using projective transformation. In fact the variables 'g' and 'h' in Eq. (10) account for this. Such perspective phenomena appear in case of viewing horizon or observing that two parallel railway tracks tend to meet at a point.

Mathematically this transformation is presented in the canonical frame as

$$\begin{pmatrix} x_c \\ y_c \\ 1 \end{pmatrix} = \begin{pmatrix} a & b & c \\ d & e & f \\ g & h & l \end{pmatrix} \begin{pmatrix} x_t \\ y_t \\ 1 \end{pmatrix}. \tag{10}$$

So eight independent parameters are required to map the contour points in the plane. The four corner points are determined to map in the canonical frame when the properties of geometrical shape can be invariantly represented. In the canonical frame the four corner points are mapped on (100, 100); (−100, 100); (−100, −100); (100, −100) coordinates.

2.2.4. Measure of goodness of fit

The measure of goodness of matching depends on the selection of control points and their mapping by fitting a function. Control points are features located in the input image and whose location in the final output is known. In the case of registration of medical images in order to force the input image to align with a reference image the control points are used. To do fit the number of control points must be greater than or equal to the number of coefficients in the polynomial. For a linear transformation as shown in Eq. (1) at least three control points are required for implementation of the mapping operation. In such cases in both medical images and satellite images a measure of goodness of fit (GOF) is achieved by the process of error minimisation. Here an error matrix termed as 'error factor e' is defined which is deduced from the difference between the predicted value and the actual value (Niblack, 1986) and which is nothing but a distance measure between the corresponding landmarks or in other words a measure of shape difference (Majumder, 1995). For each chosen concavity the best matching is searched by computing the error terms for each case

$$e = [(\partial x_m)^2 + (\partial y_m)^2]^{1/2}, \tag{11}$$

where, $\partial x_m = x'_m - x_m$ and $\partial y_m = y'_m - y_m$.

For transformation from affine to the canonical frame the control points have to be selected on a particular concavity for which the best concavity matching is achieved and the registration will be good. To match the images between each pair of contours T_1 and T_2 MR; T_1 and CT; T_2 MR and CT) we have experimented with the concavity1 (upper concavity) and concavity2 (lower concavity). From the least square solution of A and B following from the expressions where, $A = (N^TN)^{-1}N^TX$ and $B = (N^TN)^{-1}N^TY$, the coefficients of the polynomials are computed (both inner part a_0, a_1, a_2 and the higher order coefficients $a_3, a_4, a_5, a_6, \ldots$ for A and b_0, b_1, b_2 – as linear part and b_3, b_4, b_5, b_6, b_7 as non-linear part for B for the best concavity matching. The higher order terms in the polynomials are close to zero if the two shapes are mathematically similar. Following this methodology different combinations of T_1 MR, T_2 MR

and CT images are registered in affine plane and in projective plane.

3. The algorithm for matching and registration

We now describe the matching algorithm to superpose the extracted contours say C_1 and C_2 of the ROI. The transformation algorithm deforms one contour C_1 in such a way that the corresponding points in C_1 are brought nearer to the corresponding points in other contour C_2.

The computation steps are as follows:

(i) All images are brought in same dimension by proper scaling.
(ii) The boundaries of the segmented ROI (say C_1 and C_2) are extracted by Canny-edge-detector.
(iii) The edge points m_i, n_i on contour C_1 and the points o_j, p_j in the other contour C_2 are computed and are stored.
(iv) The landmark points for each contour are determined by convex hull method.
(v) For registration in the required transformation plane (affine or projective) the control points are selected searching the least square solution by minimising the expression $\|NAX\|^2$. For each concavity matching (upper or lower) and for each set of control points all the values of the polynomial coefficients and the error factor e are computed to search the best matching.
(vi) The landmark points are chosen on the upper concavity and then on the lower concavity of the contours C_1 and C_2 to re-project the contours in the canonical frame by affine transformation.

In affine plane

(vii) In affine plane for each chosen concavity, the invariant non-colinear triplets entry point e_n, exit point e_x and height point e_h Fig. 1(a) and (b) are mapped to the corresponding points (−100, 0); (100, 0) and (0, $100\sqrt{3}$) for transformation to the canonical frame.
(viii) From the generalised transformation matrix the six parameters a_0, a_1, a_2 and b_0, b_1, b_2 are computed solving six equations from the three landmark points x_1,y_1; x_2,y_2; x_3,y_3 and the three transformed coordinates x'_1,y'; x'_2, y'_2; x'_3,y'_3 where, $x'_1,y'_1 = -100,0$; $x'_2,y'_2 = 100, 0$; $x'_3,y'_3 = 0,100\sqrt{3}$. The coordinates of the $(i-3)$ points on the contour C_1 are computed in affine transformation plane from the transformation matrix and are mapped in the canonical frame. Similarly, from the three invariant triplets on the chosen concavity of the contour C_2 the rest of the points $(j-3)$ are mapped in affine plane. Thus the contours C_1 and C_2 are mapped in canonical frame and are registered.

In projective plane

(ix) In projective transformation the four corner points x_1,y_1; x_2,y_2; x_3,y_3; x_4,Y_4 of a contour are determined as landmark points by convex hull method, Fig. 1(c). Starting from the generalised transformation coordinate system the four corner points are mapped in x'_1,y'_1; x'_2,y'_2; x'_3,y'_3; x'_4,y'_4, in projective plane where $x'_1,y'_1 = -100,100$; $x'_2,y'_2 = 100,100$; $x'_3,y'_3 = 100,-100$ and $x'_4,y'_4 = -100,100$, Fig. 1(d). From mapping of the four invariant points the eight independent parameters are computed associated with the transformation matrix T. The coordinates of $(i-4)$ points of the contour C_1 are computed. Similarly the contour C_2 is mapped by projective transformation in canonical frame and the contours C_1, C_2 are registered in the projective plane.

4. Experimental results and discussion

The experiments were performed using Silicon Graphics Workstation. All images are converted from RGBA mode to grey mode in tiff format. The header is removed to convert them in raw binary version.

4.1. Preprocessing and segmentation

Preprocessing and segmentation of images are the two basic steps prior to the implementation of the shape-based methodology on the extracted contour of the ROI. We have adopted double thresholding (Canny, 1986) for region segmentation and Gaussian edge detection technique using Canny edge detector with satisfactory results. The edge detection consists of following steps:

(a) filtering, (b) enhancement, (c) detection, and (d) localisation. Filtering is performed to remove noises to improve the performance of the edge detector. The enhancement process emphasises the pixels where a significant change in local intensity values occur by computing the gradient magnitude. In detection technique the strong edge points are detected by setting proper thresholding. By the process of the localisation the location of the edge together with edge orientation are estimated. Accuracy in detection of edge location and its orientation is essential. From the edge detector a set of edge points are detected at the zero crossings of the second derivatives of the image intensity and the contour of the ROI is formed. Here the edge detector basically produces an unordered set of edges from which an ordered set is produced with the help of the algorithm. The presence of noise may result in some inaccuracy in detection of edge points. To avoid the noise effect, filtering techniques are used which combines the Gaussian filtering with the Laplacian for more accurate edge detection. To make segmentation technique more robust the threshold should be selected by the system incorporating some domain knowledge such as intensity, sizes, the number and interrelation of objects along with their probability of occurrence and distribution of intensity.

For optimal performance the following two criteria are accepted: (a) low error rate which is achieved by maximum signal to noise ratio, and (b) better localisation of the edge points (Canny, 1986). The Canny edge detection algorithm can be expressed as

$$n(x,y) = g(x,y;s) * m(x,y),$$

where the input image $m(x,y)$ is convolved by the Gaussian smoothing filter having smoothing factor s and the convolved output image array is $n(x,y)$. The output image array $n(x,y)$ consists of two arrays $a(x,y)$ and $b(x,y)$ are computed using 2×2 first difference approximations.

$$a(x,y) = \frac{[n(x,y+1) - n(x,y) + n(x+1,y+1) - n(x+1,y)]}{2},$$

$$k(x,y) = \{a(x,y)^2 + b(x,y)^2\}^{1/2}$$

gives the magnitude of the gradient. By non-maxima suppression the broad ridges of the array are thinned to get the value at the point where maximum local change occurs to identify the edge points. Double thresholding has been implemented to avoid the detection of false edges. The double thresholding algorithm is applied on the non-maxima suppressed images where the upper threshold value t_2 is chosen between $2t_1$ and $3t_1$ by trial and error to give good results. This algorithm also links the edges in a contour when it reaches the end of a contour, the algorithm looks in t_1 at the locations of the eight neighbours for edges that can be linked to the contour. The algorithm continues to gather edges from t_1 until the gap has been bridged to an edge in t_2. The tracing terminates when the current pixel is the same as the initial pixel with a closed boundary of ROI. Thus the double thresholding algorithm performs the edge linking as a by-product of thresholding.

4.2. Matching and registration

The digitised images of axial sections of the same region of the brain of an Alzheimer's patient obtained from T_1 weighted MR, T_2 weighted MR and CT modalities are used of pixel dimension 173×230. The three images under consideration are shown in Fig. 2(a) and (b) and Fig. 3. The ventricular region (ROI) is shown in Figs. 4–6. The segmented edges of the ROI using Canny edge segmentation are shown in Figs. 7–9.

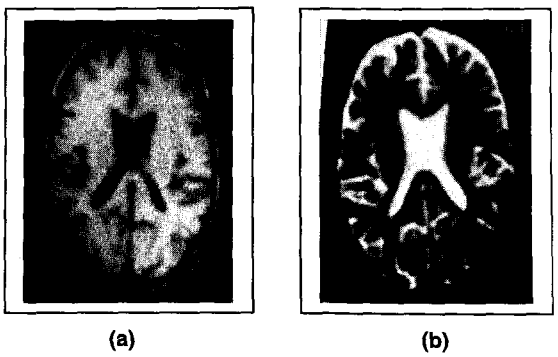

Fig. 2. (a) T_1 weighted MR image of brain of an AD patient, (b) T_2 weighted MR image of brain of the same AD patient.

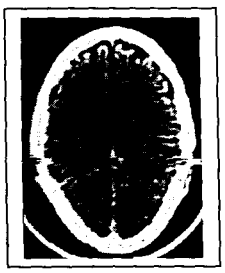

Fig. 3. CT image of brain of an AD patient.

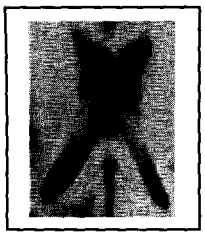

Fig. 4. Ventricular region of T_1 weighted MR image.

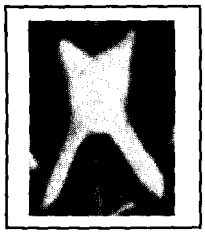

Fig. 5. Ventricular region of T_2 weighted MR image.

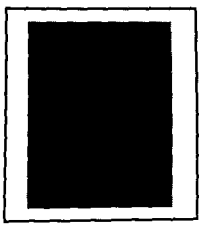

Fig. 6. Ventricular region of CT image.

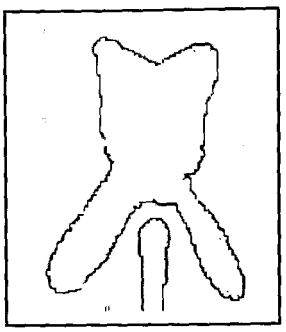

Fig. 7. Contour of the ventricle T_1 weighted MR.

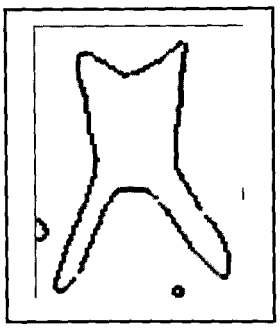

Fig. 8. Contour of the ventricle T_2 weighted MR.

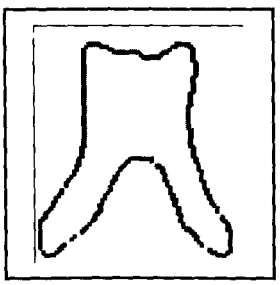

Fig. 9. Contour of the ventricle CT image.

4.2.1. Mapping of concavities in canonical frame

After edge extraction entrance, exit and heigl points of the concavities are obtained by conve hull method. These invariant points (P, Q, R MR T_1 modality are depicted on the contour (the ROI shown in Fig. 10. To map the contour i canonical frame any one of the upper or the lowe

concavities may be chosen. The affine transformation to the canonical frame is performed by mapping three points (P, Q, R) which correspond to the entrance, height and exit points of the concavity are the three vertices (−100, 0), (0, $100\sqrt{3}$,) and (100, 0) of an equilateral triangle. The point P(8.5, 9.4) corresponds to (−100, 0); point Q(42.5, 42, 5) corresponds to (0, $100\sqrt{3}$,) and point R(71.5, 3.8) corresponds to (100, 0) as shown in Fig. 10 and in Table 1. Fig. 11 shows the contour after the affine transformation. Fig. 12 depicts the superposition of ROI of T_1 MR and T_2 MR in affine plane choosing the landmark points along the lower concavity of the contour. Fig. 13 shows the invariant points on the contour of the ventricle (ROI) of T_1 weighted MR image for projective transformation and Fig. 14 depicts the mapping of the contour after projective transformation. The four invariant points are: point A(3.3, 55.5) as −100, 100; point B(94.9, 72.5) as 100, 100; point C(100.4, 6.5) as 100, −100 and point D(7.2, 16.5) as −100, −100 in canonical frame, (Table 4). Fig. 15 shows that the ROI of T_1 MR and T_2 MR are superimposed after a projective transformation. Other choices of points are also possible.

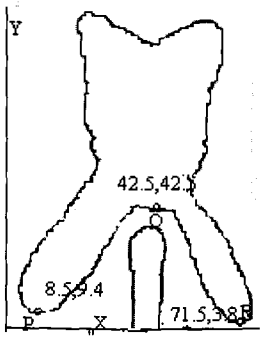

Fig. 10. The invariant points P, Q, R on the lower concavity of the contour.

Table 1
Invariant landmark points on the contour of the ventricular region of T_1 weighted MR image of brain

Upper concavity	Lower concavity	Canonical frame
3.3, 55.5	8.5, 9.4	−100.0, 0.0
15.8, 33.5	42.5, 42.5	0.0, $100\sqrt{3}$
7.2, 16.5	71.3, 3.8	100.0, 0.0

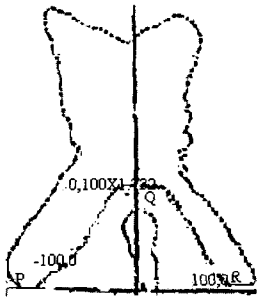

Fig. 11. Transformation of the contour in the canonical frame.

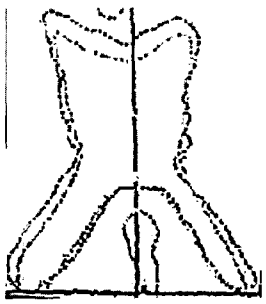

Fig. 12. Superposition of ROI T_1 MR and T_2 MR image of brain in affine plane.

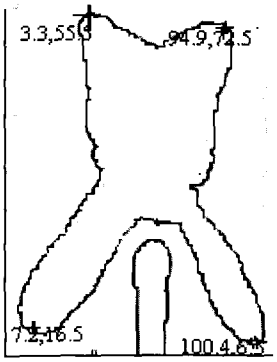

Fig. 13. Invariant points on the contour of the ventricle of T_1 MR image, projective plane.

Similarly, we have performed the registration between CT and T_1/T_2 weighted MR images. Finally the T_1 weighted MR, T_2 weighted MR and

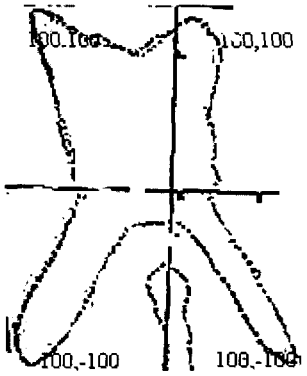

Fig. 14. Mapping of the contour in projective plane.

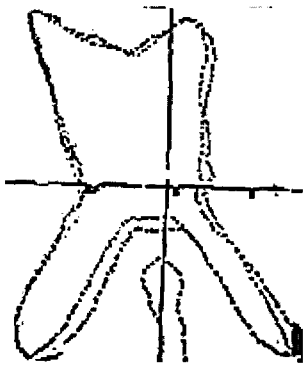

Fig. 15. Superposition of the ventricle of T_1 MR and T_2 MR in projective plane.

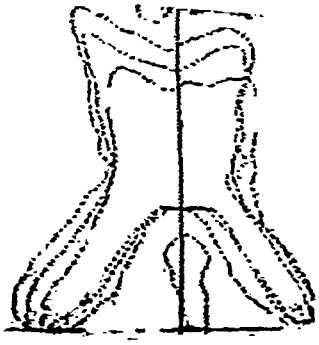

Fig. 16. Superposition of contours of ROI of T_1 MR, T_2 MR and CT in affine plane.

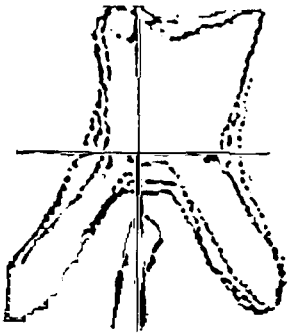

Fig. 17. Superposition of the contours of ROI of T_1 MR, T_2 and CT in projective plane.

CT images are registered in both the affine and in projective planes as shown in Figs. 16 and 17.

It is shown in Table 8 that the error factor e turns out to be smaller for the lower concavity. Hence the best matching is achieved for the control points along the lower concavity.

5. Results

Tables 2–8 show that the 'best matching' may be achieved for the selection of control points along the lower concavities.

Table 2
Invariant landmark points on the contour of the ventricular region of T_2 weighted MR image of brain

Upper concavity	Lower concavity	Canonical frame
5.4, 51.4	11.5, 7.7	−100.0, 0.0
15.5, 34.5	43.5, 41.5	0.0, $100\sqrt{3}$
7.5, 19.5	69.5, 6.5	100.0, 0.0

Table 3
Invariant landmark points on the contour of the ventricular region of CT image of brain

Upper concavity	Lower concavity	Canonical frame
8.4, 58.6	16.4, 74.5	−100.0, 0.0
12.4, 36.4	52.4, 40.5	0.0, $100\sqrt{3}$
58.4, 18.4	89.5, 3.5	100.0, 0.0

Table 4
Landmark points on the contour of ROI for the images of the three modalities (T_1 weighted MR, T_2 weighted MR and CT) in projective plane

Inv. for T_1 MR	Inv. for T_2 MR	Inv. for In CT	Inv. in canonical
3.3, 55.5	4.4, 53.5	8.4, 58.6	−100, 100
94.9, 72.5	95.4, 71.4	87.5 75.5	100, 100
100.4, 6.5	48.8, 7.5	88.9, 7.5	100, −100
7.2, 16.5	7.5, 16.5	8.4, 18.4	−100, −100

6. Conclusion

We have presented briefly the generalised theory of shape as developed by Majumder (Banerjee et al., 1995) derived the affine and projective invariance transformation relationships and applied the same to matching and registration of three sets of medical images of different modalities of the same patient suffering from Alzheimer's disease.

Table 5
Registration of T_1 MR, T_2 MR and CT images, choice of proper concavity and selection of control points on the concavity from the polynomial coefficients (a and b values)[a]

(a) Upper concavity mapping for T_1 MR image in canonical frame

Linear part

a_0	a_1	a_2	b_0	b_1	B_2
0.38	8.33	−38.5	−0.49	−0.89	50.5

Non-linear part

a_3	a_4	a_5	a_6	a_7	b_3	b_4	b_5	b_6	b_7
0.008	0.07	−0.002	0.27	−0.28	−0.037	0.085	0.18	0.19	0.19

(b) Lower concavity mapping for T_1 MR image

Linear part

a_0	a_1	a_2	b_0	b_1	B_2
−2.15	0.10	−0.06	−1.12	0.54	−0.003

Non-linear part

a_3	a_4	a_5	a_6	a_7	b_3	b_4	b_5	b_6	b_7
−0.5	−0.02	−0.07	0.07	−0.06	−0.0.3	−0.3	−0.03	−0.3	−0.3

[a]Mapping of T_1 weighted MR Image fits better in canonical frame along the lower concavity than the upper concavity as the values of the higher order polynomial coefficients are much lower for lower concavity.

Table 6
Computation of the polynomial coefficients a's and b's – the linear part and the non-linear part[a]

(a) Upper concavity mapping for T_2 MR image in canonical frame

Linear part

a_0	a_1	A_2	b_0	b_1	B_2
−0.54	0.02	0.01	−0.5	0.2	0.01

Non-linear part

A_3	a_4	a_5	a_6	a_7	b_3	b_4	b_5	b_6	b_7
0.46	0.04	−0.02	0.02	0.01	0.32	0.30	0.29	0.2	0.28

(b) Lower concavity mapping for T_2 MR image in canonical frame

Linear part

a_0	a_1	A_2	b_0	b_1	B_2
−0.04	0.12	−0.01	−0.02	0.04	−0.0

Non-linear part

a_3	A_4	a_5	a_6	a_7	b_3	b_4	b_5	b_6	b_7
1.0	−.2	−1.0	−1.1	−1.0	0.01	−0.03	−1.0	−1.0	−1.0

[a]The non-linear or the higher order coefficients have lower values for mapping of the lower concavity of the ROI of T_2 weighted MR image in canonical frame for affine transformation.

Table 7
Computation of the Polynomial co-efficients a's and b's – the linear part and the non-linear part[a]

Lower concavity mapping for CT image in canonical frame									
Linear part									
a_0	a_1	a_2	b_0	b_1	B_2				
0.04	0.12	−0.01	−0.2	0.04	−0.0				
Non-linear part									
a_3	a_4	a_5	a_6	a_7	b_3	b_4	b_5	b_6	b_7
0.34	0.06	−0.31	0.27	−0.02	−0.02	−0.02	0.07	0.22	0.23
Upper concavity mapping for CT MR image in canonical frame									
Linear part									
a_0	a_1	a_2	b_0	b_1	b_2				
−0.02	0.05	−0.65	−0.01	−0.05	−0.6				
Non-linear part									
a_3	a_4	a_5	a_6	a_7	b_3	b_4	b_5	b_6	b_7
0.01	0.2	−1.0	−1.0	−1.0	−1.0	0.8	−0.6	−0.58	−0.57

[a] The non-linear or the higher order coefficients have lower values for mapping of the lower concavity of the ROI of CT image for affine transformation.

Table 8
Error factor e_{lc} along lower concavity and error factor e_{uc} along the upper concavity of the ROI for T_1 weighted MR image, T_2 weighted MR image and for CT image of brain for AD patient

	Upper concavity	Lower concavity	Canonical frame	e_{lc}	e_{uc}
T_1 weighted MR image	3.34, 55.5	8.5,9.4	−100, 0	0.27	0.35
	15.8, 33.5	42.5, 42.5	0, 100$\sqrt{3}$		
	7.2, 16.5	71.5, 3.8	100, 0		
T_2 weighted MR image	5.4, 51.4	11.5, 7.7	−100, 0	0.28	0.57
	15.5, 34.5	43.5, 41.5	0, 100$\sqrt{3}$		
	7.5, 19.5	69.5, 6.5	100, 0		
CT image	8.4, 58.6	16.4, 74.5	−100, 0	0.28	0.31
	12.4, 36.4	52.4, 40.5	0, 100$\sqrt{3}$		
	58.4, 18.4	89.4, 3.5	100, 0		

Affine and projective transformation are used to re-project ROI into another view.

The contour matching in canonical frame is implemented using this new approach in affine and projective planes. In affine case the three landmark points and six parameters are associated by three DOF, whereas in projective case four landmark points with eight parameters and four DOF are required. A measure of GOF is implemented by the process of minimisation of an error factor.

According to experts the degeneration of an organic compound called 'myelin' occurs and causes the shape variation and enlargement due to Alzheimer's disease. Normal pressure hydrocephalus was studied by modeling brain's elastic properties in (Martin et al., 1994) to indicate the disease processes. The deformations are due to pathology and also due to the overall change in shape of the intracranial cavity of brain volume. But a comparative study of this variation in different modalities and same modality at different time will be more instructive for the clinicians. This is the view of the medical experts associated with the project.

This is a crucial point in our approach since we work by finding certain invariant points and

matching them, even if as a result of the progress in the disease conditions the structure of ROI is changed, the algorithm is general enough to capture the changes. With the change in structural (shape) properties the invariant features also may change so a re-registration will be required.

The registration process performs the integration of information from the multimodality medical imaging to a single reference frame and provides more accuracy in diagnostics procedures and improved therapeutic planning to the clinicians. All detected anatomical and functional features of the pathological growth related to ROI can be analysed simultaneously when the images are fused in a single reference frame after registration. Another important point to be noted is the detection of landmark-based concavity. The goodness of matching depends on the selection of concavity present in the images. The selection of features for recognition are view-invariant and are unaffected due to different orientation of the view. At least three control points have to be selected in a concavity to achieve a 'good fit'. If the number of control points are increased more and more polynomial coefficient would be associated, as a result the accuracy of the registration would be enhanced. An iterative process may be adopted to search the control points for best matching. From the co-registration of CT and MR images the degeneration of myelin and also the ventricular dilation can be studied properly. There are other pathological features (West et al., 1997; Canny, 1986; Arai and Kobasaki, 1983), which indicate the prognosis of AD such as the deformation of temporal horn, change in atropy and widened sulci also appear in neuroimaging. Our next attempt would be to combine all these features in a single reference frame to get necessary information of Alzheimer's disease from the fused image.

Acknowledgements

The work is part of a project jointly funded by Council of Scientific and Industrial Research (CSIR) and Department of Science and Technology (DST), Govt. of India, on knowledge-based approach in bio-medical imaging for diagnostics and therapeutic planning. We are thankful particularly to Dr. V.S. Ramamurthy, Secretary and Dr. V.K. Mishra, Advisor DST for their kind interest. The authors wish to acknowledge with thanks Dr. P. Raghunathan of All India Institute of Medical Science, Delhi, Dr. S.K. Sharma, Eko Imaging Institute, Calcutta, Dr. Goutam Ghosh, Suraksha Diagnostic Centre, Calcutta and Dr. Amitava Dutta of Kakurgachi Orthopaedic Centre, Calcutta, Dr. P.K. Roy of Burn and Standard Co. and Mr. Goutam Lohar for their valuable opinion and helpful discussions while doing the work. The authors also wish to acknowledge with thanks the help rendered by Prof. J. Das, Head, ECSU of ISI, Dr. D.P. Mukherjee, Dr. S.K. Parui, Mr. Debabrata Mitra and all other colleagues of ECSU while doing the work.

References

Arai, H., Kobasaki, K., et al., 1983. A computed tomography study of Alzheimer's disease. J. Neurol. 229, 69–77.

Banerjee, D.K., Parui, S.K., Majumder, D.D., 1994. A shape metric for 3D objects. Indian J. Appl. Math. 25, 95–111.

Banerjee, S., Mukherjee, D.P., Majumder, D.D., 1995. Point landmarks for registration of CT and MR images. Pattern Recognition Letters 16, 1033–1042.

Bhattacharya, M., Majumder, D.D., 1999. Multi resolution medical image registration using mutual information and shape theory. Accepted for Oral Presentation and in: Proc. Fourth Internat. Conf. Advances in Pattern Recognition and Digital Techniques ICAPRDT 1999, 28–31 December.

Bookstein, F.L., 1986. Size and shape spaces for landmark data in 2D. Statist. Sci. 1, 181–242.

Canny, J., 1986. A computational approach to edge detection. IEEE Trans. on Pattern Anal. Machine Intell. Pami-8 (6).

Collignon, A., Maes, F., Delaere, D., Vandermeulen, D., Suetens, P., Marchal, G., 1995. Automated image registration using information theory. In: Bizais, Y., Barillot, C., DiPaola, R. (Eds.), Proc. Information Processing in Medical Imaging. Ile de Berder, France, pp. 263–274.

Creasay, H., Schwartz, M., et al., 1986. Qualitative computed tomography in dementia of Alzheimer's type. Neurology 36, 1563–1568.

Dryden, I.L., Mardia, K.V., 1998. Statistical Shape Analysis. University of Leeds, UK, Wiley, New York.

Grimson, W.E.L., Lozano-Perez, T., Wells, W.M., Ettinger, G.J., White, S.J., Kikinis, R., 1994. An automatic registration method for frameless stereography surgery and enhanced reality visualisation. In: IEEE Proc. on CVPR, pp. 430–436.

Hill, D.L.G., et al., 1993. Registration of MR and CT images for skull base surgery using point like anatomical features. Br. J. Radiol. 64, 1030–1035.

Kendall, D.G., 1989. A survey of the statistical theory of shape. Statist. Sci. 4 (2), 87–120.

Landan, Y., Schwarts, J.T., Wolfson, H.J., 1985. Object recognition by affine invariant matching. In: Proc. CVPR, pp. 335–344.

Majumder, D.D., 1995. A study on a mathematical theory of shapes in relation to pattern recognition and computer vision. Indian J. Theoret. Phys. 43 (4), 19–30.

Majumder, D.D., Bhattacharya, M., 1997. A shape-based approach to automated screening of malignancy in tumors in tomographic and other related images. In: IETE Conf., NASELSOM-97.

Majumder, D.D., Bhattacharya, M., 1998. A new shape-based technique for classification and registration: application to multimodal medical images. Int. J. Image Process. Commun. 4 (3/4), 45–70.

Majumder, D.D., Bhattacharya, M., 1999. Cybernetic approach to medical technology for diagnosis and therapy planning. In: Proceedings of the 11th International Congress of Cybernetic and Systems organised by World Organisation of Systems and Cybernetics, August Brunel University, Uxbridge, Middlesex, West London.

Martin, J., Pentland, A., Kikinis, R., 1994. Shape analysis of brain structures using physical and experimental modes. In: IEEE Proc. on CVPR, pp. 752–755.

Medical imaging, Int. J., 1996. 6(5), 9–19.

Mukherjee, D.P., Zisserman, A., Brady, J.M., 1994. Shape from symmetry detecting and exploiting symmetry in affine images, Proc. Royal Society Series A.

Mundy, J.L., Zisserman, A., (Eds.) 1992. Geometric Invariance in Computer Vision. The MIT Press, Cambridge, MA.

Niblack, W., 1986. An Introduction to Digital Image Processing. Prentice-Hall, Englewood Cliffs, NJ.

Parui, S.K., Majumder, D.D., 1982. A new definition of shape similarity. Pattern Recognition Letter 1, 87–120.

Preparata, F.P., Ianshamos, M., 1985. Computational Geometry: An Introduction. Springer, Berlin.

Shashua, A., Navab, N., 1994. Relative affine structure : theory and application to 3d reconstruction from perspective views. In: IEEE Proc. on CVPR pp. 483–489.

Thevenaz, P., Unser, M., 1997. Spline pyramids for inter-modal registration using mutual information. In: Proceedings SPIE, Vol. 3169, pp: 236–247. Wavelet Applications in Signal and Image Processing V, San Diego, CA, July 27–August 1.

Thirion, J.P., Monga, O., Benayoun, S., Gueziee, A., Ayache, N., 1992. Automatic registration of 3D images using surface curvature. In: IEEE Int. Symp. Optical Appl. Sci. Eng., San Diego, CA, July.

Van den Elsen et.al. 1993. Medical image matching – a review with classification. IEEE Trans. Eng. Med. Bio., pp. 26–39.

Van den Elsen et.al. 1994. Automatic registration of CT and MR brain images using correlation of geometric features. IEEE Trans on Medical Imaging 14 (2), 384–398.

Well, W.M., Viola, P., Kikinis, R., 1995. Multimodal volume registartion by maximisation of mutual information. In: Proc. Med. Robot. Comp. Assist. Surg., Baltimore, pp. 52–62.

West, J., Fitzpatrick, J.M., Wang, M.Y., Dawant, B.M., Maurer, C.R., Kessler, J.R.M., Maciunas, R.J., Barillot, C., Lemoine, D., Collignon, A., Maes, F., Suetens, P., Vandermeulen, D., Van den Elsen, P.A., Napel, S., Sumanaweera, T.S., Harkness, B., Hemler, P.F., Hill, D.L.G., Hawkes, D.J., Studholme, C., Maintz, J.B.A., Viergever, M.A., Malandain, G., Pennec, X., Noz, M.E., Maguire, G.Q., Pollack, J.M., Pillazari, C.A., Robb, R.A., Hanson, D., Woods, R.P., 1997. Comparison and evaluation of retrospective intermodality brain image registration techniques. J. Comput. Assisted Tomography 21 (4), 554–566.